Available online at www.sciencedirect.com
SCIENCE DIRECT
International Journal of Pharmaceutics 307 (2006) 175–181
INTERNATIONAL JOURNAL OF PHARMACEUTICS
www.elsevier.com/locate/ijpharm

Mitoxantrone-loaded BSA nanospheres and chitosan nanospheres for local injection against breast cancer and its lymph node metastases II: Tissue distribution and pharmacodynamics

Bin Lu *, Su-Bin Xiong, Hong Yang, Xiao-Dong Yin, Ruo-Bing Zhao

West China School of Pharmacy, Sichuan University, #17, 3rd Block, Renmin South Road, Chengdu 610041, China

Received 21 June 2005; received in revised form 11 September 2005; accepted 24 September 2005
Available online 28 November 2005

Abstract

Bovine serum albumin (BSA) and chitosan (CS) nanospheres of mitoxantrone (MTO) were comparatively evaluated in terms of tissue distribution, acute toxicity and therapeutic efficiency against breast cancer and its lymph node metastases. After local injection in rats, MTO nanospheres showed a slower elimination rate and a much higher drug concentration in lymph nodes compared with MTO solution, and a lower drug concentration in other tissues. There was no observed acute toxicity to the main tissues of Kunming mice after local injection of MTO-BSA-NS. Mild toxicity to liver and lung was observed for MTO-CS-NS, but, for MTO solution, severe toxicity to liver and lung and much lower number of white blood cells were observed. Human MCF-7 breast cancer in nude mice and animal model of P388 lymph node metastases in Kunming mice were applied to investigate the therapeutic efficiency. The inhibition rate of the nanospheres against breast cancer was much higher than that of MTO solution, and lymph node metastases were efficiently inhibited by the nanospheres, especially MTO-BSA-NS.

Keywords: Mitoxantrone; Site-specific delivery; Bovine serum albumin; Chitosan; Nanospheres; Breast cancer; Lymph node metastases

1. Introduction

Breast cancer is one of the most frequently occurring cancers in women, and the second leading cause of cancer deaths in women. However, since 1989, the breast cancer morality rate has decreased 1.8% per year, due to improvements in breast cancer prevention as well as treatment (Bevers, 2001). Lymph node metastase leading to locoregional relapses is one of the decisive factors in the treatment efficiency, since lots of lymph nodes are present around the breast, especially in the armpits. Fifty to sixty percent of the breast cancer patients were detected suffering from lymph node metastases in the armpits. Even after the surgical operation, lymph node metastases are still the most serious problem that may cause secondary cancer (Li, 2000).

Mitoxantrone (MTO) is often used to treat breast cancer clinically. However, heart toxicity and myelosupression, in particular leukopenia, are its common dose limiting toxicity, and toxicity of s.c. (subcutaneous) injection was reported to be more serious than intravenous (i.v.) or intraperitoneal (i.p.) injections (Oussoren et al., 1998).

The lymphatic capillaries usually have open intercellular junctions with a size of 30–120 nm in the endothelium, which can act as channels for colloidal particles to pass into the lymphatic system. It has been demonstrated that particles less than 100 nm in size are preferable for lymph node targeting (Phillips et al., 2000). In an attempt to inhibit the primary breast cancer and to cure and prevent its lymph node metastases, MTO-BSA-NS and MTO-CS-NS with a mean size of less than 100 nm for local injection were comparatively investigated.

2. Materials and methods

2.1. Instruments, reagents and animals

Mitoxantrone (batch no. 20001009) was a gift from Sichuan Shenghe Pharmacy, China. Bovine serum albumin (Batch no. 980407, Lizhudongfeng Biotech Co. Ltd., Shanghai, China), chitosan (CS, Sigma) and other reagents of reagent grade were

DOI of original article:10.1016/j.ijpharm.2005.09.037.
* Corresponding author. Tel.: +86 28 855 02664; fax: +86 28 855 03689.
E-mail address: lubin@wcums.edu.cn (B. Lu).

0378-5173/$ – see front matter © 2005 Elsevier B.V. All rights reserved.
doi:10.1016/j.ijpharm.2005.09.038

used. MTO-BSA-NS and MTO-CS-NS were prepared and characterized in this lab. SD rats, Kunming mice (C_{57}) and BALB/c-nu nude mice were from Experimental Animal Center of Sichuan University, China.

2.2. Quantification of MTO in plasma and tissues

2.2.1. Preparation of plasma samples

SD rats were bloodlet through femoral artery. Five milliliters of the blood was taken and mixed with heparin, centrifuged at (220–350) × *g* for 10 min. To 1 ml of the supernatant was added 0.1 ml ascorbic acid–citrate buffer (0.1 M, pH 3.0). The mixture was stored at −20 °C until assay.

2.2.2. Preparation of homogenized fluids of tissues

Heart, liver, spleen, lung, kidney, axillary lymph nodes and subcutaneous tissue of the injection site of the rats were taken, respectively, washed with physiological saline, absorbed dry with a filter paper. To a weighed portion of each tissue 0.5 ml water and 50 μl ascorbic acid–citrate buffer (0.1 M, pH 3.0) were added, and the mixture homogenized.

2.2.3. Quantification of MTO

0.5 ml plasma sample or homogenized sample was mixed with 0.2 ml methanol, 0.2 ml formic acid, 0.1 ml 20% (w/v) trichloroacetic acid and 0.4 ml chloroform in a polypropylene tube, vortexed for 3 min, centrifuged at 1600 × *g* for 10 min, and the supernatant kept in refrigerator. The supernatant was centrifuged at 1600 × *g* for 10 min again before assay and 10 μl used for HPLC. The conditions for HPLC were: chromatograph column C3 (300 mm × 6 mm i.d., 5 μm), protection column Phenomenex ODS guard cartridge (4.0 mm × 3.0 mm i.d.), column temperature 35 °C, mobile phase methanol–0.16 M ammonium formate (48:52, pH 2.7), flow rate 1.0 ml/min, wavelength for detection 658 nm (the maximum absorption wavelength in the mobile phase).

2.3. Tissue distribution

Fifty-four SD rats were divided randomly into 18 groups, each group 3 rats. Six groups received s.c. injection of MTO-BAS-NS and six groups of MTO-CS-NS at 5 mg MTO/kg dose level, another six groups for the control, MTO solution (designated MTO-Soln) at the same dose level. The rats of each group were sacrificed by femoral arteriotomy 1, 4, 12, 24, 72 and 120 h after administration, respectively, and then dissected, each time one group of MTO-BAS-NS, MTO-CS-NS and MTO-Soln being treated. The injection site (subcutis), axillary lymph nodes, heart, liver, spleen, lung and kidney were taken, absorbed dry with a filter paper, weighed and stored at −20 °C. Quantification of MTO was carried out according to Section 2.2.

2.4. Tests for acute toxicity

2.4.1. Determination of LD_{50}

One hundred and fifty Kunming mice, weighing 18–22 g, were divided randomly into 15 groups, 10 mice each group. Five groups were used for MTO-BSA-NS, five groups for MTO-CS-NS and another five groups for MTO-Soln. Subcutaneous injection of the same volume of the drug was conducted at 1.6, 5.1, 7.3, 10.5 and 15 mg MTO/kg dose level, respectively (dose ratio being 0.7:1, one dose level for each group). The mice were observed for 14 days, and the toxicity symptoms and death numbers recorded. LD_{50} with 95% confidence was calculated.

2.4.2. Body weight change

During the time period of the above experiment, body weight of the mice was recorded. The mean body weight changing with time was plotted.

2.4.3. Count of while blood cells and pathological examination

MTO-BSA-NS, MTO-CS-NS and MTO-Soln were each injected s.c. to 50 Kunming mice at 8 mg MTO/kg dose level. Bloodletting was conducted after 72 h of injection through orbit, and the white blood cells counted. The mice were dissected and tissues (skin of the injection site, lymph nodes, heart, liver, spleen, lung, kidney, stomach and intestine) taken, fixed with 4% formaldehyde, embedded with paraffin wax, sliced, stained by HE method and examined under microscope.

2.5. Pharmacodynamic study

2.5.1. Establishment of the model of human MCF-7 breast cancer

Cultivation and augmentation of human MCF-7 breast cancer cells were conducted as described in the literature (Chamras et al., 2002). The cells were adjusted to 1×10^7 ml^{-1}.

Six to eight-week-old BALB/c-nu nude mice were inoculated of human MCF-7 breast cancer cells under the breast at a dose level of 0.2 ml of 1×10^7 ml^{-1} per mouse. When the tumor phymata grew to a certain volume, the mice were sacrificed and the phymata taken and cut into cubes of 2 mm edge length. Twenty-four BALB/c-nu nude mice (aged 6–8 weeks) were implanted with the phyma cube under the breast.

2.5.2. Inhibition tests on human MCF-7 breast cancer

A week later when the tumor grew normally, the mice were divided randomly into four groups, six mice each group. The first group received s.c. injection close to the tumor with MTO-BSA-NS (1.0 mg MTO/kg dose level), the second group with MTO-CS-NS (1.0 mg MTO/kg dose level), the third group with MTO-Soln (2.0 mg MTO/kg dose level), and the fourth group with physiological saline 0.04 ml per mouse. The administration continued for successive seven times with an s.c. injection every 4 days. Four days after the last administration, the mice were sacrificed and dissected. The tumor phymata were weighed, and the major diameter (d_1) and minor axis (d_2) measured. The volume of the tumor phyma was calculated according to the equation $(\pi d_1 d_2^2)/6$. The tumor inhibition rate was calculated based on the tumor weight of the drug group and the weight of the blank

group:

$$\text{Inhibition rate} = \left(1 - \frac{W_{\text{drug}}}{W_{\text{blank}}}\right) \times 100\%$$

The pathological slices of the tumor phyma were examined under microscope.

2.5.3. Establishment of the model of lymph node metastases with P388 cells and tests on inhibition of lymph node metastases

Liquid nitrogen-frozen P388 cells were defrozen quickly at 37 °C, washed three times with physiological saline and centrifuged at 150 × *g* for 10 min each time. The cells in the bottom suspension were counted under microscope. Three Kunming mice were inoculated i.p. with 0.4 ml cell suspension and raised until 9 days when a large amount of ascites formed. The ascites were taken and counted for P388 cells and diluted with physiological saline to make a work suspension of 2.16×10^9 cells/ml.

To each of 40 female Kunming mice, 0.05 ml work suspension was injected s.c. at claw pat of the left posterior limb (Hagiwara et al., 1996). On day 7 after inoculation, the mice were divided randomly into four groups, 10 mice each group. One group received s.c. injection of MTO-BSA-NS at 1.0 mg MTO/kg dose level at claw pat of the left posterior limb, the second group of MTO-CS-NS at 1.0 mg MTO/kg dose level, the third group of MTO-Soln at 2.0 mg MTO/kg dose level and the fourth group of 0.04 ml physiological saline (blank). After 30 days of observation, the mice were sacrificed. Lymph nodes behind the geniculum were taken, their diameter measured and volume calculated. Pathological slices of the normal lymph nodes, of the lymph nodes with P388 cells and of the lymph nodes with P388 cells after s.c. injection of the drug were compared under microscope.

3. Results and discussion

3.1. Quantification of MTO in plasma and tissues

MTO was reported to be not stable enough in physiological saline or biological samples. It was suggested that antioxidants be added and polypropylene vessel used to reduce adsorption (Hu, 1990). In our experiments, ascorbic acid was used as the antioxidant, trichloroacetic acid as the precipitation agent for protein, formic acid for increasing the solubility and extraction efficiency of MTO and chloroform for preventing from oily layer formation which might make sampling difficult.

3.1.1. Optimizaton of the extraction procedures

The amount of methanol, the variety and amount of the acid used in extraction were optimized, while other components had been optimized and kept unchanged [0.1 ml 20%, w/v, trichloroacetic acid and 0.4 ml chloroform], with lung homogenates as the extraction model. When extraction was carried out without any acids, the extraction efficiency was only 3.72%. When HCl was used, 6 M HCl could not give repeatable results, while 1 M HCl could be used only for multiple-extraction, otherwise the extraction efficiency was very low. When formic acid was used instead of HCl, results were much better, and the best result was: 0.2 ml methanol and 0.2 ml formic acid, which gave an absolute extraction efficiency of (89.97 ± 2.61)% ($n = 3$) when extracted once. The absolute extraction efficiencies obtained for plasma, heart, liver, spleen, kidney, lymph node and subcutis were 98.53 ± 2.28%, 79.52 ± 5.80%, 61.65 ± 5.89%, 51.95 ± 3.93%, 74.50 ± 6.23%, 68.79 ± 6.57% and 89.41 ± 4.22% (mean ± S.D., $n = 3$), respectively. These amounts of methanol and formic acid were adopted as the routine procedure as described in Section 2. Multi-extraction was not used to save time because of the large number of samples to be assayed. In the literature, the absolute extraction efficiencies of over 50% were considered as feasible, and on very few conditions, an absolute extraction efficiency as low as 38% was also employed (Rentsch et al., 1996).

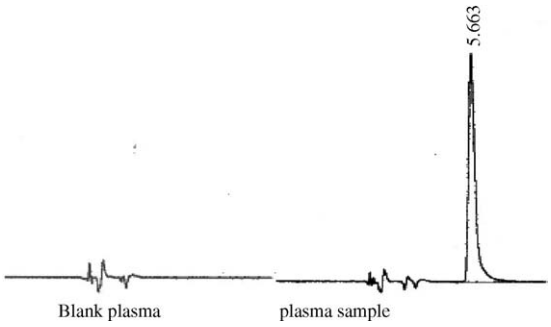

Fig. 1. HPLC chromatograms of plasma showing separating MTO from other coexisting materials.

3.1.2. Standard regression equations for the calibration curves

Phosphorous pentoxide-dried MTO (10 mg) was added to methanol with 0.5 g ascorbic acid and made 100 ml as the stock solution, which was diluted with methanol to make work solutions. 0.5 ml blank plasma sample or blank tissue homogenate was mixed with 0.2 ml MTO work solution of different concentrations. Each 0.5 ml of the mixtures was treated and determined with HPLC as described in Section 2. All the HPLC chromatograms showed that the MTO peaks separated well with the peaks of foreign substances, as shown in Fig. 1. The detection limit was 10 ng/ml when signal/noise = 3.0. The standard regres-

Table 1
Standard regression equations of mitoxantrone in plasma/tissue homogenates

Samples	Linear range (ng/ml or ng/g)	Regression equations	*r*
Plasma	49.956–2997.36	$A = 14.056C - 485.77$	0.9999
Heart	49.956–2997.36	$A = 15.28C + 612.87$	0.9998
Liver	99.912–2997.36	$A = 7.2533C + 254.89$	0.9991
Spleen	99.912–2997.36	$A = 7.0473C - 140.72$	0.9997
Lung	49.956–2997.36	$A = 12.087C - 156.96$	0.9999
Kidney	49.956–2997.36	$A = 10.402C - 581.95$	0.9993
Lymph node	49.956–2997.36	$A = 9.007C - 166.11$	0.9996
Subcutis	49.956–2997.36	$A = 11.917C - 186.98$	0.9992

Table 2
MTO remained in the subcutis of injection and its absorption percentages after s.c. of MTO-BSA-CN, MTO-CS-NS and MTO-Soln ($n = 3$)

Time (h)	Remained in the subcutis (μg)			Percentages absorbed (%)		
	MTO-BSA-CN	MTO-CS-NS	MTO-Soln	MTO-BSA-NS	MTO-CN-NS	MTO-Soln
1	193.35 ± 12.74	533.37 ± 151.11	151.70 ± 13.07	74.41 ± 2.93	24.24 ± 5.41	78.82 ± 1.22
4	139.75 ± 333.67	320.48 ± 53.92	102.17 ± 44.22	81.97 ± 4.35	56.95 ± 14.75	87.80 ± 6.42
12	122.51 ± 19.71	219.08 ± 42.98	96.66 ± 44.02	81.77 ± 3.02	70.88 ± 4.76	86.97 ± 5.07
24	74.56 ± 15.72	170.34 ± 25.22	85.78 ± 31.20	81.77 ± 1.79	76.15 ± 2.55	87.83 ± 4.64
72	75.96 ± 36.69	162.11 ± 37.97	57.84 ± 17.79	89.94 ± 4.97	78.88 ± 4.81	93.12 ± 0.64
120	50.54 ± 23.46	122.30 ± 41.61	36.48 ± 18.78	93.17 ± 2.03	82.75 ± 3.55	95.85 ± 0.32

sion equations obtained are shown in Table 1. Should samples contain MTO over the concentration range, the samples were assayed again after dilution.

3.1.3. Recoveries and precision for quantification of MTO in plasma and tissues

Low, medium and high amounts of MTO were added to the biological samples and relative recoveries and precision determined based on Table 1. The recovery results were all in the range of 98.24–101.65% with a R.S.D. of 1.96–5.55%. The within-day R.S.D. was in the range of 0.49–5.73% and between-day R.S.D. in the range of 2.02–9.71%.

3.2. Tissue distribution

3.2.1. MTO remained in the subcutis of injection and its absorption percentage

MTO-BSA-NS or MTO-CS-NS could remain in the injection site for a long time but were absorbed slowly, while MTO-Soln eliminated and absorbed much faster, as shown in Table 2. The results indicated that the nanospheres showed a sustained release behavior and supplied the drug as a reservoir. This might favor the longer therapeutic efficiency and smaller side-effects.

3.2.2. Time courses of MTO concentration in the tissues

The time courses of MTO concentration in the tissues after s.c. injection are shown in Table 3.

For MTO-BSA-NS and MTO-CS-NS, the MTO concentration in axillary lymph nodes was much higher than other tissues for almost all time periods (MTO-BSA-NS at 4 h in kidney was the only exception), which was a strong indication of the lymph node targeting characteristic of these two nanospheres. T_{max} in axillary lymph nodes for these two nanospheres was both around 24 h, which was the same for MTO-Soln. C_{max} of axillary lymph nodes was 35.25 μg/g for MTO-BSA-NS and 22.11 μg/g for MTO-CS-NS and 12.77 μg/g for MTO-Soln μg/g, which were all higher than C_{max} of any other tissues and indicated that, not only these two nanosphers, but also MTO itself showed a tendency of lymph node targeting. MTO-BSA-NS showed the best targeting characteristic for lymph nodes.

3.3. Tests for acute toxicity

LD_{50} was not improved by microencapsulation compared with MTO-Soln, as listed in Table 4. The main cause of death was gastrointestinal flatulence and diarrhea, which resulted in loss of appetite. Gastrointestinal toxicity of MTO was also reported in the literature (Schaich et al., 2002).

Table 3
Time courses of MTO concentration (μg/g) in the tissues after s.c. of MTO-BSA-NS, MTO-CS-NS and MTO-Soln ($n = 3$)

Time (h)		Axillary lymph nodes	Heart	Liver	Spleen	Lung	Kidney
1	MTO-BSA-NS	4.99 ± 6.88	0.66 ± 0.13	1.11 ± 0.08	1.31 ± 0.09	1.15 ± 0.17	3.11 ± 0.67
	MTO-CS-NS	3.13 ± 1.88	0.23 ± 0.03	0.31 ± 0.11	0.50 ± 0.04	0.40 ± 0.03	1.27 ± 0.16
	MTO-Soln	2.88 ± 0.97	1.18 ± 0.15	1.93 ± 0.20	2.23 ± 0.25	1.96 ± 0.20	5.44 ± 0.90
4	MTO-BSA-NS	6.51 ± 4.82	1.60 ± 0.39	3.59 ± 0.37	3.70 ± 0.52	1.71 ± 0.10	6.90 ± 0.23
	MTO-CS-NS	7.28 ± 1.57	0.89 ± 0.79	1.36 ± 0.59	1.07 ± 0.43	0.80 ± 0.23	3.47 ± 1.62
	MTO-Soln	3.20 ± 0.66	1.68 ± 0.08	2.85 ± 0.47	3.08 ± 0.74	1.93 ± 0.11	6.82 ± 0.64
12	MTO-BSA-NS	34.80 ± 17.55	2.67 ± 0.72	4.41 ± 0.42	4.85 ± 1.75	3.18 ± 0.42	12.30 ± 1.95
	MTO-CS-NS	15.63 ± 20.91	1.02 ± 0.34	1.65 ± 0.13	2.07 ± 0.47	1.36 ± 0.30	4.30 ± 0.89
	MTO-Soln	8.76 ± 10.36	3.20 ± 1.06	3.16 ± 0.77	3.95 ± 2.24	2.33 ± 0.19	7.34 ± 5.88
24	MTO-BSA-NS	35.25 ± 12.25	2.21 ± 0.70	3.41 ± 1.39	7.09 ± 1.09	2.88 ± 0.66	9.51 ± 3.70
	MTO-CS-NS	22.11 ± 24.47	1.44 ± 0.35	2.06 ± 0.83	3.10 ± 0.67	1.79 ± 0.82	5.49 ± 1.24
	MTO-Soln	12.77 ± 1.30	2.57 ± 0.73	3.42 ± 0.93	6.90 ± 3.87	2.44 ± 1.03	8.82 ± 4.07
72	MTO-BSA-NS	29.30 ± 21.75	2.19 ± 1.10	3.26 ± 1.72	8.19 ± 1.86	3.09 ± 0.30	8.15 ± 3.78
	MTO-CS-NS	13.63 ± 6.37	1.79 ± 0.57	1.90 ± 1.01	5.27 ± 3.40	2.64 ± 0.92	8.59 ± 3.29
	MTO-Soln	10.47 ± 9.16	2.41 ± 0.69	3.07 ± 1.60	11.40 ± 3.71	3.42 ± 0.19	10.54 ± 3.05
120	MTO-BSA-NS	27.09 ± 37.52	1.47 ± 0.09	1.78 ± 0.61	7.52 ± 3.68	2.91 ± 0.96	7.55 ± 0.93
	MTO-CS-NS	5.07 ± 1.43	1.35 ± 0.46	1.16 ± 0.19	4.30 ± 1.83	1.55 ± 0.75	4.55 ± 0.51
	MTO-Soln	2.32 ± 0.37	2.04 ± 1.10	1.33 ± 0.84	7.35 ± 1.07	2.50 ± 1.50	7.74 ± 3.06

Table 4
LD_{50} values and number of white blood cells counted 72 h after s.c. injection

Preparations	No. of mouse	LD_{50} (mg/kg)		WBC $\times 10^{9}$[a] (l^{-1})
		7 days	14 days	
MTO-BSA-NS	50	8.5 ± 1.6	5.9 ± 1.5	13.10 ± 7.66
MTO-CS-NS	50	8.8 ± 1.7	4.8 ± 0.9	8.96 ± 2.18
MTO-Soln	50	10.5 ± 2.0	5.9 ± 1.1	7.56 ± 2.82

[a] The value of the normal mice being $(12.61 \pm 5.28) \times 10^{9}\ l^{-1}$.

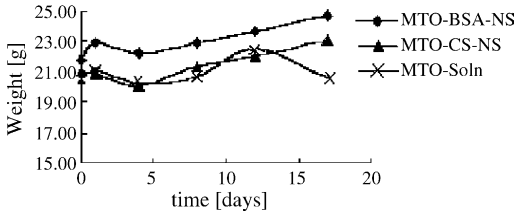

Fig. 2. Time courses of average mouse body weight after s.c. injection.

The time courses of average body weight of the mice after s.c. injection are shown in Fig. 2. For MTO-CS-NS, the time course of body weight almost coincided with that of MTO-Soln, the only difference being that in the final days (after day 13) MTO-CS-NS showed a better body weight. The time course for MTO-BSA-NS was more satisfactory than that of MTO-Soln, which indicated that the acute toxicity of MTO-BSA-NS was lower.

Number of white blood cells counted 72 h after administration was also listed in Table 4, which is another indication that MTO-BSA-NS showed lower acute toxicity.

Pathological slices showed that, for MTO-BSA-NS, no pathological change was observed for all tissues examined, including the gastrointestinal tract. While for MTO-CS-NS, liver denaturation of low-grade and interstitial pneumonia were observed. But, for MTO-Soln, medium to serious hepatonecrosis and interstitial pneumonia were observed.

3.4. Pharmacodynamic study

3.4.1. Tumor inhibition tests on human MCF-7 breast cancer

A preliminary test was first conducted in an attempt to cause primary breast cancer. Six to eight-week-old BALB/c-nu nude mice were inoculated of human MCF-7 breast cancer cells under the breast at 0.2 ml of $1 \times 10^{7}\ ml^{-1}$ per mouse dose level. The cancer phyma began to form 14 days after inoculation, and the

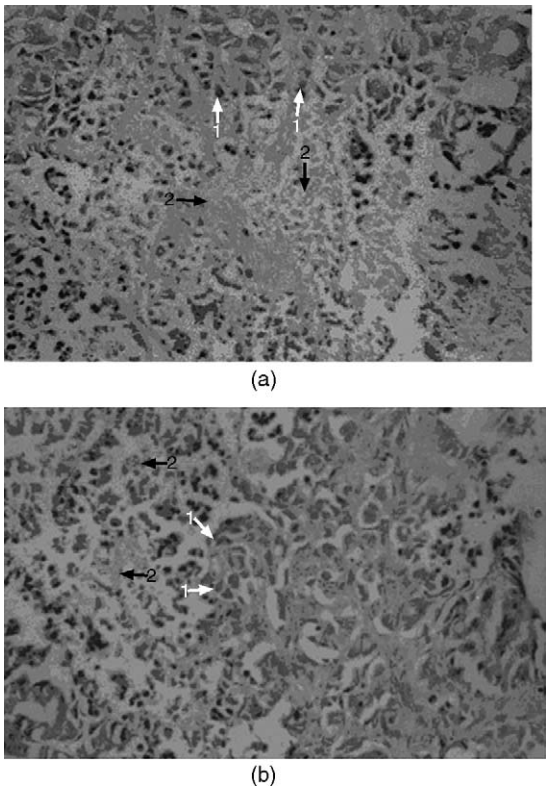

Fig. 3. Pathological slice microscopy of MCF-7 breast cancer with s.c. injection of MTO-BSA-NS or MTO-CS-NS (a) and physiological saline (b). Arrows 1 pointing to living MCF-7 cells in the overgrown layer; arrows 2 pointing the necrosed MCF-7 cells.

cancer phyma increased to a certain volume after 1 month. But the volumes were different from one mouse to another, which was difficult for further evaluation of tumor inhibition. Hence, the method to form primary cancer was given up, and the procedures in Section 2 were adopted using cancer phyma cubes to form secondary breast cancer. The size of the breast cancer and inhibition rate after administration are compared in Table 5.

Taking the difference of dose level between MTO nanospheres and MTO-Soln group into account, one can conclude that, MTO-BSA-NS and MTO-CS-NS, especially the latter, gave better therapeutic efficiency than MTO-Soln, especially the size of the tumor was considered.

It is interesting that on the surface of the tumor phyma treated by the nanospheres a thin layer of blue coat could be observed, which is an indication that MTO-BSA-NS and MTO-CS-NS have a strong affinity to the tumor tissue, and without doubt the coat might reinforce the therapeutic efficiency of the antitumor

Table 5
The size of the breast cancer and its inhibition rate in different groups ($n = 6$)

Groups	MTO dose (mg/kg)	Tumor size (mm^3)	P^*	Inhibition rate (%)	P^*
MTO-BSA-NS	1.0	67.67 ± 41.91	$P_1 < 0.10$, $P_2 > 0.35$, $P_3 < 0.0064$	77.65 ± 10.98	$P_1 > 0.29$, $P_2 > 0.43$
MTO-CS-NS	1.0	30.81 ± 13.94	$P_2 > 0.29$, $P_3 < 0.0051$	83.91 ± 4.12	$P_2 > 0.94$
MTO-Soln	2.0	46.88 ± 31.52	$P_3 < 0.0066$	82.86 ± 11.13	
Blank	0	351.23 ± 163.89		0	

* P_1, compared with MTO-CS-NS; P_2, compared with MTO-Soln; P_3, compared with the blank.

Table 6
Lymph node size of mice after s.c. injection of P388 cells with and without injection of MTO preparations ($n = 10$)

Preparations	MTO dose (mg/kg)	Lymph node size (mm^3)	P^*
MTO-BSA-NS	1.0	26.67 ± 14.55	$P_1 > 0.10$, $P_2 < 0.05$, $P_3 < 0.01$
MTO-CS-NS	1.0	62.63 ± 39.84	$P_2 > 0.10$, $P_3 < 0.05$
MTO-Soln	2.0	119.32 ± 57.30	$P_3 > 0.20$
Blank	0	186.83 ± 77.71	

* P_1, compared with MTO-CS-NS; P_2, compared with MTO-Soln; P_3, compared with the blank.

agent. For MTO-Soln, no blue coat on the tumor surface could be observed.

The pathological slice photos of human MCF-7 breast cancer are shown in Fig. 3. In the center of the tumor phyma, necrotic spots were present. For MTO nanospheres, overgrowth layer of the tumor was very thin or even absent, but the overgrowth layer looked obviously thick for the MTO-Soln group.

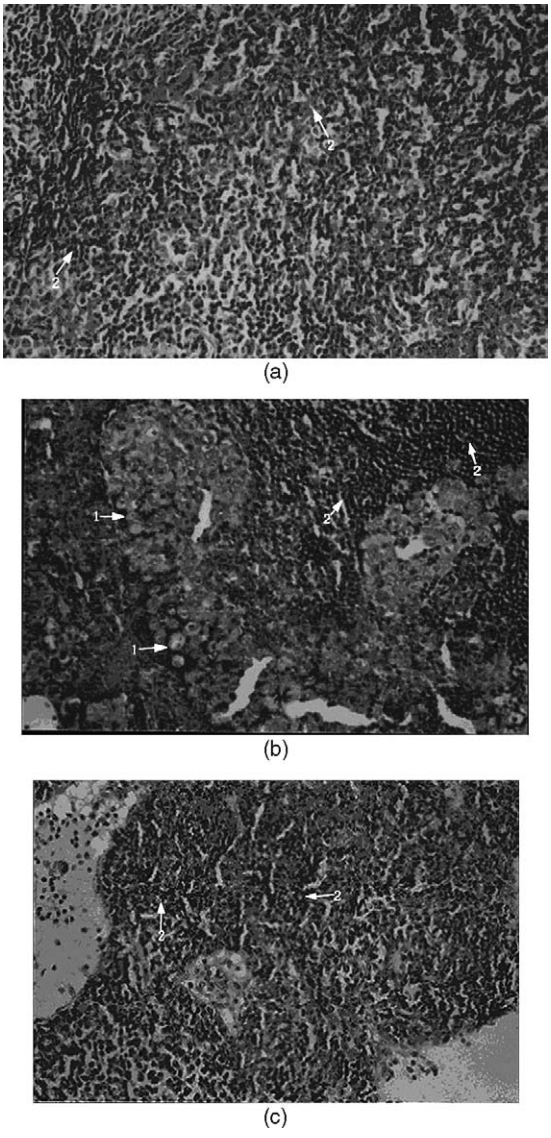

Fig. 4. Pathological slice microscopy of normal lymph node (a), lymph node with P388 cells (b) and lymph node with P388 cells after s.c. injection of MTO nanospheres (c). Arrows 1 pointing to P388 cells; arrows 2 pointing to lymph node cells.

3.4.2. Lymph node metastases and their inhibition

Since there were no reports in the literature about the model of lymph node metastases of breast cancer, melanoma cells were used to establish this model, according to the literature (Kata et al., 1982). However, establishment of lymph node metastase model with melanoma cells was unsuccessful: when C_{57} mice were used for inoculation under the breast, no lymph node metastases were observed until the mice were all dead. P388 cells, according to the literature (Hagiwara et al., 1996), were then used. The microscopic photos of pathological slices of the normal lymph nodes, of the lymph nodes with P388 cells (the saline control) and of the lymph nodes with P388 cells after s.c. injection of MTO nanospheres are shown in Fig. 4. The establishment of the model of lymph node metastases with P388 cells proved successful, as seen from a comparison of Fig. 4(a–b), and the inoculation was 100% successful. The P388 cells were much less in Fig. 4(c), indicating the therapeutic efficiency of MTO-BSA-NS and MTO-CS-NS against lymph node metastases.

The results of lymph node size measurement are listed in Table 6. The difference between MTO-BSA-NS and MTO-Soln, or MTO-BSA-NS and the blank or MTO-CS-NS and the blank was significant; while that between MTO-BSA-NS and MTO-CS-NS, or between MTO-CS-NS and MTO-Soln or between MTO-Soln and blank was insignificant. Considering that the dose level was different between MTO nanospheres and MTO-Soln, the inhibition effect of MTO-BSA-NS for lymph node metastases was much better, and that of MTO-CS-NS was better than that of MTO-Soln. It has been reported that lymph node metastases of breast cancer may happen before or after the appearance of the breast cancer niduses. The statistical data of 2491 breast cancer patients in China showed that the 10-year-fraction surviving was 68% for patients with negative axillary lymph node metastases, 40.1% for patients with 1–3 positive axillary lymph nodes, 31.4% for 4–7 positive axillary lymph nodes, and only 13.2% for patients with over eight positive axillary lymph nodes (Li, 2000). MTO nanospheres against both breast cancer and its lymph node metastases must benefit the improvement of clinical efficiency.

4. Conclusions

The major features of our MTO nanospheres were: (1) a high efficiency in the targeting of the drug into lymph nodes; (2) a strong affinity to tumor tissues (a coat layer of MTO-BSA-NS or MTO-CS-NS was observed concentrating on the surface of tumors), which must benefit the therapeutic efficiency of antitumor agents.

MTO-BSA-NS showed much lower toxicity than MTO-Soln and also lower than MTO-CS-NS. The therapeutic efficiency of MTO-BSA-NS and MTO-CS-NS against breast cancer and lymph node metastases was better than MTO-Soln, with MTO-CS-NS superior to MTO-BSA-NS against human MCF-7 breast cancer and MTO-BSA-NS superior to MTO-CS-NS against lymph node metastases of P388 cells. Considering safety as the primary criteria, we may conclude that, as a whole, MTO-BSA-NS were superior to MTO-CS-NS.

The results showed that nanospheres seem to be a promising carrier system for tumor agents to breast cancer and especially for its lymph node metastases.

References

Bevers, T.B., 2001. Breast cancer chemoprevention: current clinical practice and future direction. Biomed. Pharmacother. 55, 559–564.

Chamras, H., Ardashian, A., Heber, D., Glasy, J.A., 2002. Fattic acid modulation of human MCF-7 breast cancer cell proliferation, apoptosis and differentiation. J. Nutr. Biochem. 13, 711–716.

Hagiwara, A., Takahashi, T., Sawai, K., 1996. Methotrexate bound to carbon particles used for treating cancers with lymph node metastases in animal experiments and a clinical pilot study. Cancer 78, 2199–2209.

Hu, O.Y.P., 1990. Novel assay method for mitoxantrone in plasma and its application in cancer patients. J. Chromatogr. 532, 337–350.

Kata, A., Takakura, Y., Hashida, M., 1982. Physico-chemical and antitumor characteristics of high molecular weight prodrugs of mitomycin. Chem. Pharm. Bull. 36, 2951–2957.

Li, S.L. (Ed.), 2000. Oncology of Mammary Gland. Publishing House of Science and Technology, Beijing, pp. 1–134.

Oussoren, C., Eling, W.M.C., Crommelin, D.J.A., 1998. The influence of the route of administration and liposome composition on the potential of liposomes to protect tissue local toxicity of two antitumor drugs. Biochim. Biophys. Acta 1369, 159–172.

Phillips, W.T., lipper, R.K., Goins, B., 2000. Novel method of greatly enhanced delivery of liposomes to lymph nodes. J. Parmacol. Exp. Ther. 295, 309–313.

Rentsch, K.M., Schwendener, R.A., Haeseler, E., 1996. Determination of mitoxantrone in mouse whole blood and different tissues by high-performance liquid chromatography. J. Chromatogr. 679, 185–192.

Schaich, M., Illmer, T., Aulitzky, W., 2002. Intensified double induction therapy with high dose mitoxantrone, etoposide, *m*-amsacrine and high dose ara-C for elderly acute myeloid leukaemia patients aged 61–65 years. Haematologica 87, 808–815.